Final Report: A computational model for glycogenolysis in skeletal muscle

By Melissa J. Lambeth and Martin J. Kushmerick

Grayson Gerlich and Alexa Schwartz

Abstract

Glycogenolysis and glycolysis are key metabolic pathways used to generate energy rich molecules for muscular contractions. When transitioning from rest to maximal strain, the ATP flux in skeletal muscle cells can change by two orders of magnitude [1]. This remarkable activity—along with the importance of musculature in everyday life—makes the skeletal muscle glycolysis pathway an inviting target for study. Lambeth and Kushmerick modeled this system in 2002, and were able to demonstrate a high dependence on ATPase and the concentration of inorganic phosphorus (Pi) in the system utilizing fractional factorial design (FFD) analysis. However, since then, FFD analysis resolution has improved significantly due to available computing power, and more experimental data on enzyme kinetics in human muscle has become available. To improve the results of this influential study, we 1) update kinetic parameters from human skeletal muscle, and 2) perform higher resolution FFD analysis on the updated model.

Introduction

Glycolysis is a highly conserved metabolic pathway that generates energy storage molecules for cells across all domains of life. Glycolysis utilizes glucose to form pyruvic acid and utilizes the release of free energy to form adenosine triphosphate (ATP) and reduced nicotinamide adenine dinucleotide (NADH). In Eukaryotic cells, products from glycolysis are often transported into the mitochondrion for further use in the Krebs cycle. In mammalian muscle cells, ATP can be used for muscular contractions. Cells store ATP from aerobic respiration during rest, but can generate extra ATP by anaerobic glycolysis if needed during intense contractions. The glucose produced for glycolysis comes from the breakdown of glycogen through a process called glycogenolysis.

Glycogenolysis and glycolysis occur through a host of enzymatic transitions controlled by feedback inhibition, and are therefore intriguing systems to model. Glycolysis is key to cell health in many different organ systems in humans (ie. muscle, liver) and malfunction of glycolysis has been linked to diseases such as diabetes and cancer [9,10]. In 2002, few modeling efforts had been completed for mammalian muscular glycogenolysis and glycolysis, but other models were complete in fungi and bacteria species. Flux and regulation within glycolysis seems closely tied to the type of cell that experiments are conducted in. Lambeth and Kushmerick identified a gap in the understanding of glycolysis in muscle, and aimed to

re-evaluate work done to model glycolysis in muscle from 1968. Key issues they identified in modeling glycolysis in muscle at the time are: 1) dynamic flux of ATP; 2) variability caused by muscle properties and intensity of contractions; 3) uncertainty in enzyme kinetics; and 4) disagreement within the research community regarding flux control mechanisms.

Summary of Study

Methods

Enzyme kinetics for glycogenolytic enzymes were compiled from literature, and a basic model was constructed to include reactions from glycogen to lactate with the inclusion of adenylate kinase and creatine kinase (Figure 1). This model was constructed as an isolated pathway to characterize only internal functions, therefore external addition or consumption of substrates, and external regulation of enzymes were not evaluated. Michaelis-Menten kinetics were used to describe fluxes within the system based on *in vitro* enzyme experiments from previous literature. Literature values were obtained from a variety of muscle cell samples including chicken, mouse, rat, rabbit, pig, and human. All enzymes were modeled with reversible kinetic equations to determine whether rapid-equilibrium assumptions were reasonable.

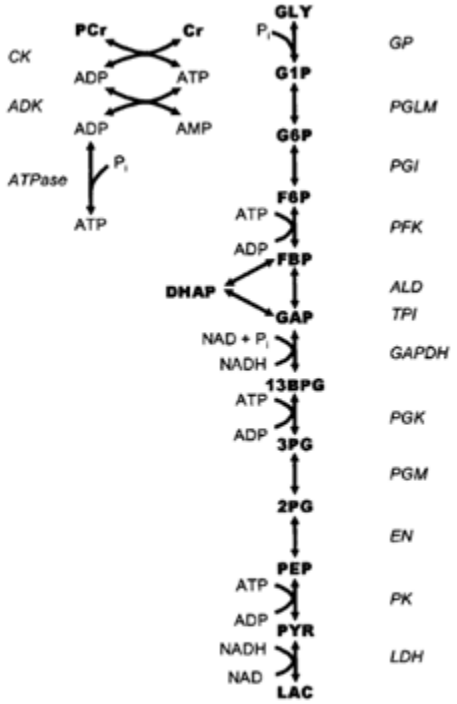

FIGURE 1. Schematic representation of all reactions used in the model.

Kinetic equations were chosen based on known in vitro enzyme behavior and could be grouped into allosteric or rapid equilibrium bi-bi groups. Equation 1 shows the Michaelis-Menten kinetics used for bi-bi reactions when affinity binding constants were unavailable in literature.

$$V = \frac{\frac{V_{\max f} AB}{K_a K_b} - \frac{V_{\max r} PQ}{K_p K_q}}{1 + \frac{A}{K_a} + \frac{B}{K_b} + \frac{AB}{K_a K_b} + \frac{P}{K_p} + \frac{Q}{K_q} + \frac{PQ}{K_p K_q}}.$$

Equation 1. Michaelis-Menten Kinetics of bi-bi reactions.

Because the system was modeled as a closed system, internal Haldane modifications were used without needing to adjust the parameters to preserve thermodynamics within the system. This allowed for the thermodynamic constant K_{eq} to be incorporated into the model for each enzymatic transition. The Haldane modification is shown in equation 2.

$$V_{\max \text{ reverse}} = \frac{V_{\max \text{ forward}} K_{m\text{reverse}}}{K_{m\text{forward}} K_{\text{eq}}}.$$

Equation 2. Haldane modification calculated with Keq.

The system was run under three different conditions to simulate three different contraction states within the muscle cells. Resting cells had a low ATP flux, moderate exercise had mid level ATP flux, and intense exercise had high ATP flux. The flux from phosphate containing species for each exercise state is shown in table 1.

Table 1. Flux concentrations of phosphate containing species based on exercise intensity.

Physiological State	Rest (mM)	Moderate exercise (mM)	Maximal exercise (mM)
ATPase coefficient	0.075	0.75	7.5
ATP flux (mM/min)	0.6	6.1	58.4
ATP	8.2	8.2	7.8
ADP	0.0078	0.032	0.415
AMP	3.3E-6	5.7E-5	0.010
P_i	0.64	7.1	31.5
PCr	32.8	28.6	3.0
NAD/NADH	513	12	1

A sensitivity analysis was performed on the model by perturbing each enzyme Vmax by 1% with the exclusion of ATPase. Initial concentrations of each metabolite were also analyzed via 1% perturbation. This analysis was supplemented with an FFD analysis by simulating each

metabolite at their physiological maxima and minima concentrations to determine which species had the greatest effect on formation of the final product.

Results

The model generated from the 12-enzyme system (right side of Figure 1) produced a steady state where the net flux of the system goes to zero. Mass action ratios were used to validate the model and resulted in consistent values compared to equilibrium constants applied to the model, with the resulting values agreeing with experimental data within the experimental accuracy. The model was used to generate Figure 2 as substrates reach equilibrium over time. The results show depletion of the glycogen stores going to lactate, and reaching equilibrium as inorganic phosphate (Pi) reaches a depleted concentration.

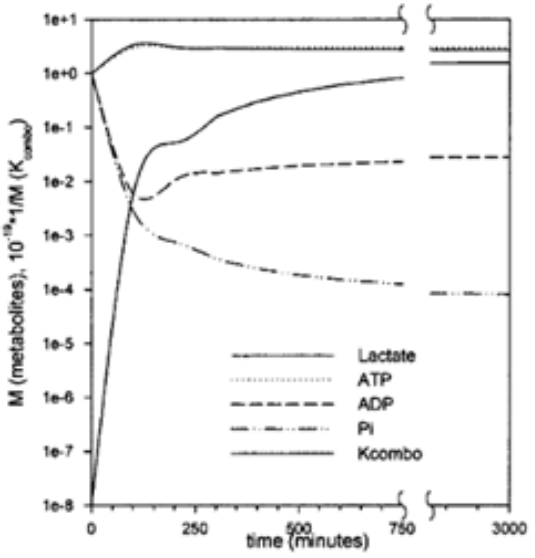

FIGURE 2. Approach of metabolites towards equilibrium. Initial conditions are standard (1 M) for all metabolites. $K_{eqcombo}$ (M^{-1}) is multiplied by 10^{-19} for visual purposes.

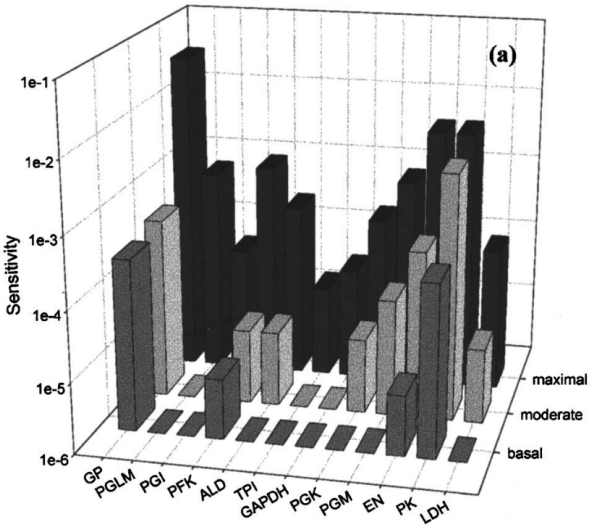

Figure 3. Sensitivity analysis of enzymes

From these results, the model was modified to demonstrate a better steady-state result for mammalian muscle cells. The glycogen was assumed to be constant (infinite store of glycogen), the lactate was allowed to sink infinitely, and an ATPase was added to the system to free inorganic phosphate from ATP. With these modifications, the model was used to achieve steady state, however the flux of the system became dependent on the flux of ATPase, because the system was directly affected by the conservation of Pi through ATP and ADP. These results highlighted the importance of Pi on the overall flux of the system, and the relative unimportance of glycogen and lactate concentration. It was determined that ATPase exerts 95% control over the system, therefore it was excluded from the sensitivity analysis of other enzymes in the system.

The sensitivity analysis performed on each enzyme highlighted the variability in behavior based on exercise intensity (Figure 3). Glycogen phosphorylase, phosphofructokinase, and pyruvate kinase showed the most control over the system at rest and low exercise, while other enzymes showed very little control over the system until simulated at intense exercise. From this analysis, the conclusion can be drawn that at high exercise, control mechanisms other than phosphate availability become important. The FFD analysis further confirmed that inorganic phosphate concentration was crucial to the system behavior, but also indicated the importance of ADP. In fact, utilizing FDD analysis indicated a greater importance of ADP than the sensitivity analysis alone (Table A1, Figure A2).

Limitations

The authors identify that using kinetic values from *in vitro* experiments is not ideal, and modeling should be done with *in vivo* values when experimentally available. As well, utilizing only human skeletal muscle kinetic values would improve consistency of resulting data. Some of the values utilized for resting muscle were not obtained from muscular samples, and therefore those values should also be updated. The authors simplify an equation for bi-bi reactions due to a lack of information on random binding patterns at the time of publication. A portion of the bi-bi systems have been investigated since 2002, making those simplifications unnecessary in future analysis. The FFD analysis is also poorly described, leading to uncertainty about the role of multifactor effects.

Modernizing the Model

Methods

The first step to updating the model by Lambeth and Kushmerick was to find in vivo kinetic parameters for human skeletal muscle enzymes. Updated values are shown in table 2. Availability of data for these parameters remains somewhat limited due to modern experimentation focusing largely on conditions pertaining to disease. These values were not used because they did not represent healthy muscular contraction conditions.

Table 2. Updated parameters from human skeletal muscle.

Enzyme	Parameter	Original		Updated	Ref
Glycogen Phosphorylase A	K_{GLYf}	1.7	Rabbit	2.3	2
	K_{G1P}	2.7	Rabbit	2.8	3
Glycogen Phosphorylase B	K_{iPi}	4.6	Rabbit	5.1	3
	K_{G1P}	1.5	Rabbit	2.8	3
	K_{iGLYb}	4.4	Rabbit	4.2	3
Phosphofructokinase	K_{ADP}	2.71	Rabbit	2.31	4
Aldolase	K_{FBP}	0.05	Rabbit	0.027	5
	K_{DHAP}	2.1	Rabbit	2.38	4
	K_{GAP}	1.1	Rabbit	0.7	5
Triose phosphate isomerase	K_{GAP}	0.32	Rabbit	0.34	6
	K_{DHAP}	0.61	Human	0.61	1,6
Enolase	K_{2PG}	0.12	Rat	1.41	4
Pyruvate kinase	K_{PYR}	7.05	Rabbit	13.3	4
Lactate dehydrogenase	K_{LAC}	17	Mouse	15.7	4
Creatin kinase	K_{iATP}	3.5	Rabbit	3.3	7
	K_{iADP}	0.135	Rabbit	0.67	7

With updated parameters in hand, we recreated the model as published by Lambeth and Kushmerick in COPASI [8]. Although Lambeth and Kushmerick provide an exhaustive list of model parameters and equations, there were a point of confusion, namely the lack of a cited K_{eq} value for adenylate kinase (commonly called myokinase) which is required to calculate a reverse reaction rate using the Haldane relation. We were able to find numerous values for the adenylate kinase equilibrium constant in contemporary literature and we averaged these to select a proper value. In COPASI, the model is represented entirely in one compartment with 22 species and 16 reactions.

We verified the presence of a steady state at all three flux levels by integration. All time course simulations were performed with a relative tolerance of 1e-6, and an absolute tolerance of 1e-12. Production runs were generally done with 2400 intervals over chosen timescales with the LSODA solver, although 20000 intervals were used for a high-resolution run to confirm the validity of other results (data not shown). The RADAU solver (also used by Lambeth and Kushmerick) was used for comparison and was nearly 100x slower, indicating a significant increase in efficiency with the more modern LSODA solver.

Flux control coefficients were determined using COPASI's Metabolic Control Analysis function. Sensitivity analysis was done by perturbing each initial concentration by 1% and observing the effect of these perturbations on the overall reaction flux. The 2^{8-4} fractional factorial design

analysis was performed in Minitab with automatic principle fraction generation. Other data was plotted using Excel.

Results

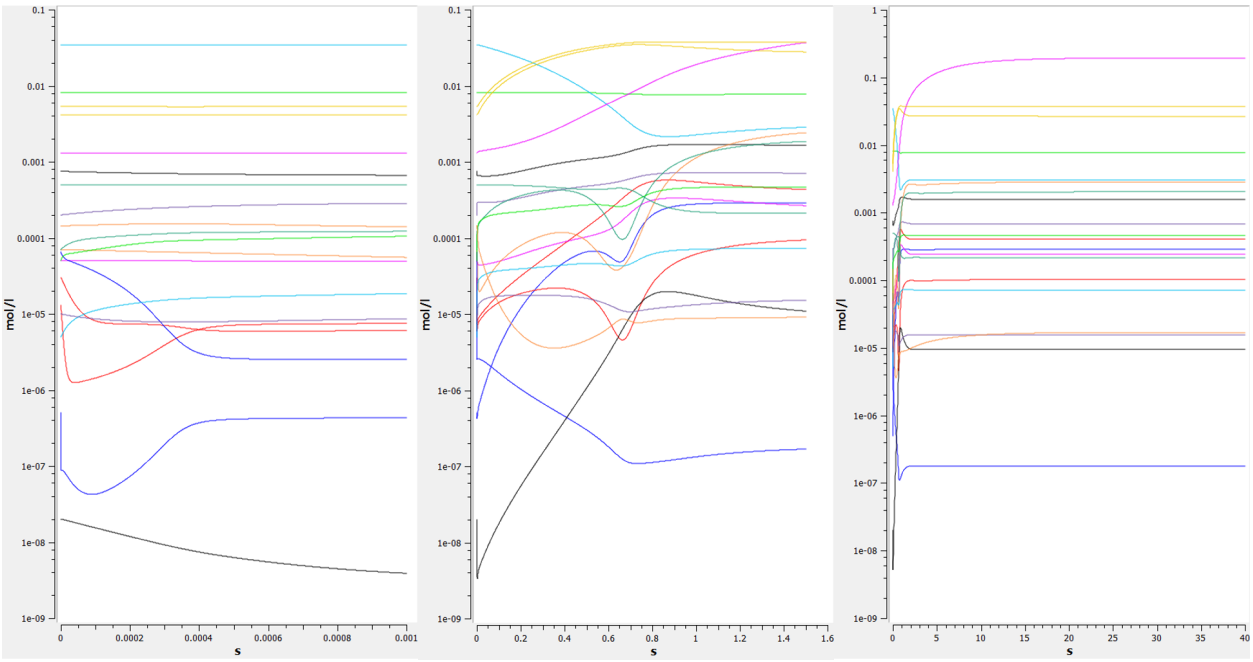

Figure 4: Plots of substrate concentrations (log mol/l) vs time (s) for production runs of the model. Each run was performed with 2400 intervals using the LSODA algorithm. Left: 1 millisecond of simulation time. Center: 1.5 seconds of simulation time. Right: 40 seconds of simulation time.

Lambeth and Kushmerick do not thoroughly describe model dynamics and only plot model activity in the context of thermodynamic validation. As a result, the behavior of the model is not well characterized. At all levels of ATP flux, we observed three separate timescales of notable activity as demonstrated in Figure 4. The first is a short timescale, almost all complete within one millisecond, where enzymes close to equilibrium and those with very rapid reactions quickly adjust from their initial concentrations. The second timescale, mostly within one second, is the one with both the most interest and most relevance. Muscle contractions occur quickly, and there is significant dynamism in place within the pathway to respond to sudden action, especially at high intensity. The final timescale, mostly within 20 seconds, characterizes the final, slow progression of several metabolites, notably lactate and pyruvate, to their steady state values. This is also physiologically reflected as the buildup of lactate in the muscles lags behind the onset of high activity.

With the model verified, we proceeded to perform a sensitivity analysis. The first analysis was performed with 1% perturbations of enzyme V_{max} values and visualized as flux control coefficient

data shown in Figure 5.

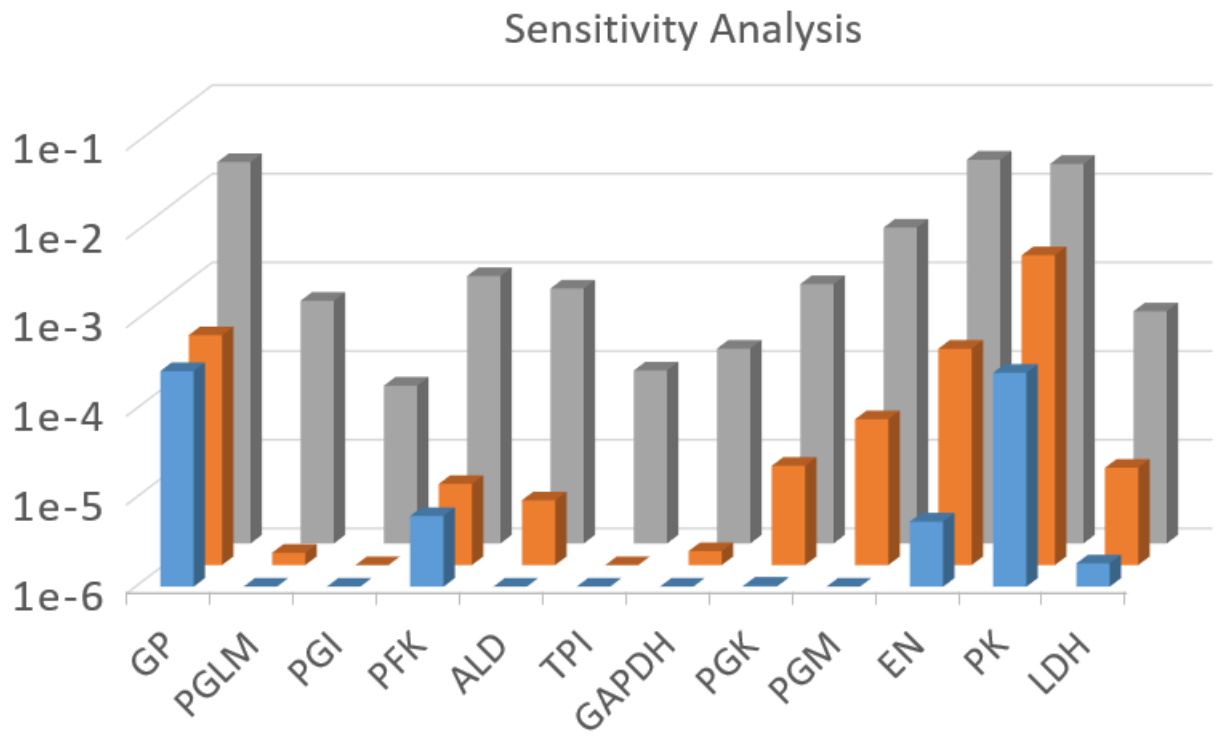

Figure 5: Sensitivity analysis with respect to enzyme V_{max} values. Blue shows rest conditions, orange shows moderate exercise, gray shows maximal exercise.

As per Lambeth and Kushmerick, ATPase, which exerts 95% of the pathway control, was not considered in this analysis. Our sensitivity analysis follows the same trends as the one from the prior model, as we expected. Our updated model elucidates some nuances missed by Lambeth and Kushmerick, largely in the form of small scale (1e-6) flux controls at lower ATP fluxes. Of particular interest, however, are aldolase (ALD) and triose phosphate isomerase (TPI), which both show order-of-magnitude increases in their flux control under maximum ATP flux. Both of these enzymes received mostly updated parameter values during our modernization. Therefore, we can conclude that even relatively minor changes in parameter values can have significant effects on model behavior, highlighting the importance of such modernization. Additionally, the importance of glycogen phosphorylase (GP) relative to enolase (EN) and pyruvate kinase (PK) is decreased at high ATP flux vs Lambeth and Kushmericks model. This further reinforces the control switching mechanism that helps the glycolysis pathway transition from a system driven by Pi to one driven by secondary factors.

In order to inform our fractional factorial design (FFD) analysis, we performed a series of sensitivity analyses to determine the effects of 1% perturbations of initial substrate conditions on total pathway flux.

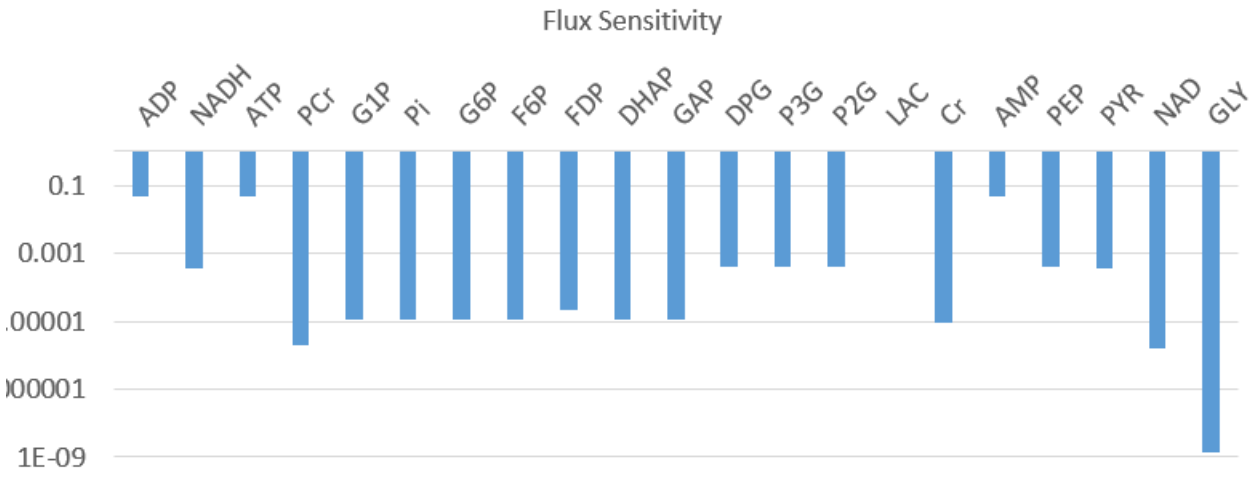

Figure 6: Plot of a sensitivity analysis testing the sensitivity of total reaction flux to perturbations of initial conditions under maximal ATP flux.

As shown in figure 6, many of the parameters are inherently linked by stoichiometry to have the same effects on overall pathway flux. As a result, it would be computationally wasteful to determine the effects of all of them. As such, we do not have the requisite degree of complexity to perform a FFD of resolution V, which would ensure that two-factor effects are unconfounded by other two-factor effects. In order to achieve this resolution, we would need to strive for either a full fractional design, or perhaps an FFD of resolution VI, either of which would require more than 100 different production runs. Therefore, we chose to run a 2^{4-8} FFD analysis (detailed in table 3) including the same species included by Lambeth and Kushmerick for comparison.

Table 3: Results from our FFD analysis. Results larger than Lambeth and Kushmerick's data are highlighted in green, while those lower are highlighted in red. All of the values changed slightly, but those highlighted represent the most significant.

ADP	**Pi**	**PCr**	**LAC**	**AMP**	**G6P**	**NADH**	**GLY**
1.61e-4	1.11e-6	3.94e-6	4.02e-6	1.86e-5	3.50e-6	1.55e-6	4.76e-6
ADP:Pi		**PCr:LAC**		**AMP:G6P**		**NADH:GLY**	
6.9e-4		3.8e-6		1.2e-6		9.2e-7	

Although the results are largely in the same order of magnitude as those from Lambeth and Kushmerick, there is a notable increase in several factors. Perhaps most interesting are the increase in the mixed effects from ADP:Pi and PCr:LAC. The first, coupled with the relative lack of increase in the main effect from ADP, further confirms the importance of ADP in control switching. Although there was a marked increase in the main effect of Pi, the decreased

sensitivity to GP at maximal ATP flux shows that the effect of PCr:LAC is also contributing to control switching more than previously determined.

The final point of interest in the FFD data is the decreased effects of both NADH and GLY. The physiological implication of this result is unclear, but it may indicate the greater pathway has more independence from glycogenolysis than previously indicated by the model.

Limitations and Future Considerations

Despite some improved availability of experimental data in human skeletal muscle, there are still kinetic values that are still not available from in vivo human samples. Obtaining these kinetic values may yet provide a more accurate picture of enzyme control of glycolysis. Modeling glycolysis in only three physiological conditions is a vast oversimplification of the extreme range of conditions muscles can achieve during contractions, recovery, and rest. Ideally, models could be modified based on relevant experimental data to simulate a variety of different muscular behaviors. Finally, this model utilizes the simplicity of a fully reversible and closed system, when in fact, lactate efflux would realistically change the behavior of the entire system. Further research into this model might benefit from considering lactate as a dynamic metabolite.

Conclusions

Through this study, we aimed to modernize the Lambeth and Kushmerick model and explore the capabilities of the updated model. Using modern solvers, the efficiency of the model was increased drastically, allowing for quick iteration and comparison of production runs. Our sensitivity analysis revealed an increased role of secondary factors during maximal exercise, as well as the importance of such modernization efforts in accurate model characterization. Our FFD analysis further reinforced the importance of ADP in control switching and demonstrated a reduced effect of glycogen on pathway flux. Overall, it is a fair claim that the updated model reveals nuances missed by Lambeth and Kushmerick's original model while further solidifying the role of key enzymes in the control switching mechanism that allows glycolysis to sustain its wide range of physiological ATP fluxes.

References

1. Lambeth, Melissa. Kushmerick, Martin. “A Computational Model for Glycogenolysis in Skeletal Muscle”. *Annals of Biomedical Engineering*. **30**. 808-827. (2002)

2. Rush, James. Spriet, Lawrence. “Skeletal muscle glycogen phosphorylase a kinetics: effects of adenine nucleotides and caffeine”. *J Appl Physiol*. **91**. 2071-2078. (2001)

3. Nikos G Oikonomakos, Vicky T Skamnaki, Erzsébet Ösz, László Szilágyi, László Somsák, Tibor Docsa, Béla Tóth, Pál Gergely. “Kinetic and Crystallographic Studies of Glucopyranosylidene Spirothiohydantoin Binding to Glycogen Phosphorylase b”. *Bioorganic & Medicinal Chemistry*.**10**. 261-268. (2002)

4. Wiśniewski JR, Gizak A, Rakus D. “Integrating Proteomics and Enzyme Kinetics Reveals Tissue-Specific Types of the Glycolytic and Gluconeogenic Pathways”. *J Proteome Res*.**14**. 3263-3273. (2015)

5. Eagles, Peter. Iqbal, Muzaffar. “A Comparative Study of Adolase from Human Muscle and Liver” *Biochem J.* **133**. 429-439. (1973).

6. Dabrowska A, Kamrowska I, Baranowski T. Purification, crystallization and properties of triosephosphate isomerase from human skeletal muscle. *Acta Biochim Pol*. **25**. 247-256. (1978)

7. Lee, C. Nicholson, G. O’Sullivan, W. “Some Properties of Human Skeletal Muscle Creatine Kinase” *Aust J Biol Sci*. **30**. 507-517. (1977).

8. Hoops S., Sahle S., Gauges R., Lee C., Pahle J., Simus N., Singhal M., Xu L., Mendes P. and Kummer U. COPASI: a COmplex PAthway SImulator. *Bioinformatics* **22**, 3067-74 (2006).

9. Xin Guo, Honggui Li, Hang Xu, Shihlung Woo, Hui Dong, Fuer Lu, Alex J. Lange, Chaodong Wu. “Glycolysis in the control of blood glucose homeostasis” Acta Pharmaceutica Sinica B. **2**. 358-367. (2012)

10. Adewale Fadaka, Basiru Ajiboye, Oluwafemi Ojo, Olusola Adewale, Israel Olayide, Rosemary Emuowhochere. “Biology of glucose metabolization in cancer cells”. Journal of Onological Sciences. **3**. 45-51. (2017)

Appendix A: supplemental tables and figures

Table **A1**. Original FFD results

TABLE 6. Design matrix for 2_{IV}^{8-4} fractional factorial design analysis.

Run	P_i	AMP	ADP	NADH	PCr	GLY	G6P	LAC
1	−	−	−	+	+	+	−	+
2	+	−	−	−	−	+	+	+
3	−	+	−	−	+	−	+	+
4	+	+	−	+	−	−	−	+
5	−	−	+	+	−	−	+	+
6	+	−	+	−	+	−	−	+
7	−	+	+	−	−	+	−	+
8	+	+	+	+	+	+	+	+
9	+	+	+	−	−	−	+	−
10	−	+	+	+	+	−	−	−
11	+	−	+	+	−	+	−	−
12	−	−	+	−	+	+	+	−
13	+	+	−	−	+	+	−	−
14	−	+	−	+	−	+	+	−
15	+	−	−	+	+	−	+	−
16	−	−	−	−	−	−	−	−
Main effects	7.64E-07	1.65E-05	1.59E-04	1.72E-06	4.24E-06	5.03E-06	2.78E-06	4.33E-06
17	+	+	+	+	+	−	−	+
18	+	+	+	+	+	−	+	−
19	+	+	+	+	+	+	−	−
20	+	+	+	+	+	+	+	+
Mixed effects	ADP:P_i 5.2e-4	PCr:LAC 3.4e-6	AMP:G6P 1.1e-6	NADH:GLY 1.0e-6				
	Largest mixed effect consists of ADP:P_i, AMP:G6P, GLY:NADH, PCr:LAC							

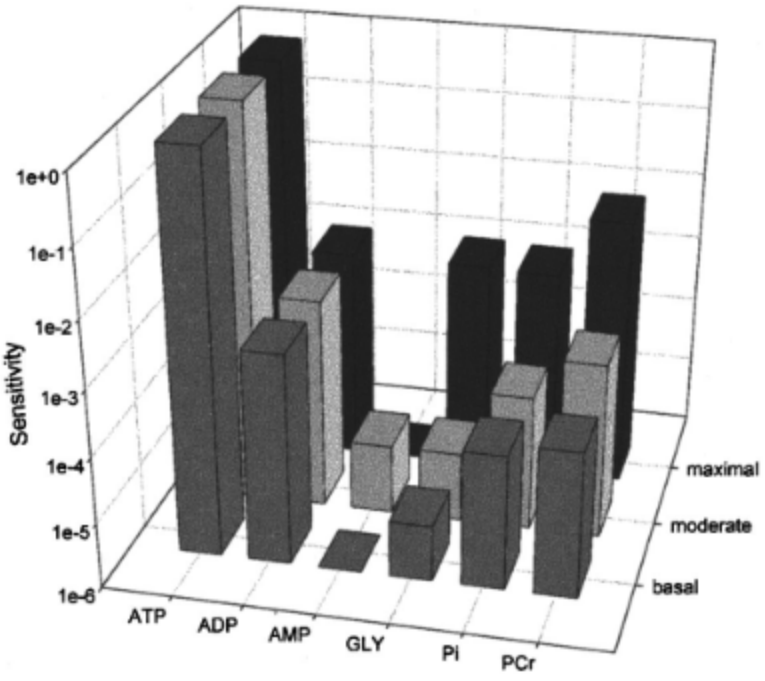

Figure A2. Sensitivity analysis of metabolites at three exercise intensities.